



**Mediterranean sea  
level response to  
atmospheric  
pressure**

P. Oddo et al.

This discussion paper is/has been under review for the journal Geoscientific Model Development (GMD). Please refer to the corresponding final paper in GMD if available.

# Sensitivity of the Mediterranean sea level to atmospheric pressure and free surface elevation numerical formulation in NEMO

P. Oddo<sup>1</sup>, A. Bonaduce<sup>2</sup>, N. Pinardi<sup>1,2,3</sup>, and A. Guarneri<sup>1</sup>

<sup>1</sup>Istituto Nazionale di Geofisica e Vulcanologia, Bologna, Italy

<sup>2</sup>Centro EuroMediterraneo per I Cambiamenti Climatici, Bologna, Italy

<sup>3</sup>Università degli Studi di Bologna, Dipartimento di Fisica e Astronomia, Bologna, Italy

Received: 5 March 2014 – Accepted: 16 April 2014 – Published: 18 June 2014

Correspondence to: P. Oddo (paolo.oddo@bo.ingv.it)

Published by Copernicus Publications on behalf of the European Geosciences Union.

Title Page

Abstract

Introduction

Conclusions

References

Tables

Figures



Back

Close

Full Screen / Esc

Printer-friendly Version

Interactive Discussion



## Abstract

The sensitivity of the dynamics of the Mediterranean Sea to atmospheric pressure and free surface elevation formulation using NEMO (Nucleus for European Modelling of the Ocean) was evaluated. Four different experiments were carried out in the Mediterranean Sea using filtered or explicit free surface numerical schemes and accounting for the effect of atmospheric pressure in addition to wind and buoyancy fluxes. Model results were evaluated by coherency and power spectrum analysis with tide gauge data. We found that atmospheric pressure plays an important role for periods shorter than 100 days. The free surface formulation is important to obtain the correct ocean response for periods shorter than 30 days. At frequencies higher than  $15 \text{ days}^{-1}$  the Mediterranean basin's response to atmospheric pressure was not coherent and the performance of the model strongly depended on the specific area considered. A large amplitude seasonal oscillation observed in the experiments using a filtered free surface was not evident in the corresponding explicit free surface formulation case which was due to a phase shift between mass fluxes in the Gibraltar Strait and at the surface. The configuration with time splitting and atmospheric pressure always performed best; the differences were enhanced at very high frequencies.

## 1 Introduction

The Mediterranean Forecasting System (MFS, Pinardi and Flemmings, 1989) started in the late 1980s during the years of growing interest in the operational framework of applied marine science. It now provides real-time environmental information about the Mediterranean Sea with continuously growing accuracy. The modelling component of the MFS is the focus of the present study.

The Ocean General Circulation Model (OGCM), which solves the primitive equations and integrates observational information for analyses and forecasts, has been enhanced continuously over the past 15 years. The evolution of the model can be

GMDD

7, 3985–4017, 2014

## Mediterranean sea level response to atmospheric pressure

P. Oddo et al.

Title Page

Abstract

Introduction

Conclusions

References

Tables

Figures



Back

Close

Full Screen / Esc

Printer-friendly Version

Interactive Discussion



## Mediterranean sea level response to atmospheric pressure

P. Oddo et al.

Title Page

Abstract

Introduction

Conclusions

References

Tables

Figures



Back

Close

Full Screen / Esc

Printer-friendly Version

Interactive Discussion



traced back by referring to the related literature (Demirov and Pinardi, 2002; Oddo et al., 2009). The current operational model consists of a NEMO (Madec, 2008) based code, under incompressible and hydrostatic approximation, with  $1/16^\circ$  horizontal resolution, 72 vertical levels with partial cells, fully accounting for the air–sea fluxes by dedicated bulk formulae, connected to the global model (Drevillon et al., 2008). It also takes into account the fresh water input from the major Mediterranean rivers (details on the implementation of the model can be found in Oddo et al., 2009).

The NEMO code solves a prognostic equation for the sea surface elevation, and the induced external gravity waves (EGW) are currently treated using a filter approach developed by Rouillet and Madec (2000) which allows for longer time-step saving computational time. In version 3.3, the time-splitting technique was introduced into the NEMO code according to Griffies (2004), allowing for an explicit representation of the EGW.

The sea level and its variability have a strong social and economical impact which explains the growing interest worldwide in the correct estimate of their evolution and variability, both in time and space. The Mediterranean Forecasting System is one example of the considerable effort spent in trying to achieve such accuracy.

In the open ocean the response of the sea level to atmospheric pressure is close to the inverse barometer (IB) effect (Wunsch, 1972; Ponte, 1993) and thus, for a long time, the atmospheric pressure effect has been not explicitly implemented in numerical ocean models. The classical IB approximation formulates the static response of the ocean to atmospheric pressure forcing. The validity of this IB assumption depends on the time and space scales considered: the ocean response to atmospheric pressure generally differs from the IB for periods less than three days and at high latitudes. However in closed or semi-enclosed seas, such as the Mediterranean, the response is more complex.

Sea-level variations in the Mediterranean Sea at time scales from one to ten days have been shown to be primarily due to surface pressure changes related to synoptic atmospheric disturbances (Kasumovic, 1958; Mosetti, 1971; Papa, 1978; Godin and Trotti, 1975). On the other hand, sea-level variations at lower time scales have been

## Mediterranean sea level response to atmospheric pressure

P. Oddo et al.

Title Page

Abstract

Introduction

Conclusions

References

Tables

Figures

◀

▶

◀

▶

Back

Close

Full Screen / Esc

Printer-friendly Version

Interactive Discussion



explained as due to atmospheric planetary waves (Orlic, 1983). It has been also observed that a significant departure from a standard IB effect can occur at frequencies higher than 30 days<sup>-1</sup> (Le Traon and Gauzelin, 1997). Departures from the IB response may be due to either local winds (Palumbo and Mazzarella, 1982) or to the restrictions at straits on water transport between basins (Garret, 1983; Garrett and Majaess, 1984). Crepon (1965) has also shown that the response of a rotating fluid is never barometric. It may be quasi-barometric if the space scale of the atmospheric disturbance is smaller than the barotropic radius of deformation. He also showed that the larger the bottom friction, the closer the response to barometric pressure. Coastlines that can support Kelvin waves cause barometric adjustments. Atmospheric pressure driven flows through the Mediterranean straits lead to mass, momentum and vorticity exchanges between the connecting basins (Candela and Lozano, 1994).

It is thus clear that the dynamics of the Mediterranean Sea forced directly and indirectly by atmospheric pressure cover a large spectrum of processes with different temporal and spatial scales. We thus believe that the sensitivity of the dynamics induced by atmospheric pressure to the numerical formulation used to solve the surface elevation equation is an important area for investigation.

Section 2 describes the pressure formulation adopted in NEMO, together with the numerical schemes implemented to solve the sea level equation. Details on the NEMO implementation and experimental set up are described in Sect. 3. Model simulation results of the Mediterranean response to the atmospheric pressure and sensitivity to the numerical scheme used to solve the sea level equation are discussed in Sect. 4. Section 5 provides a summary and conclusions.

## 2 The pressure formulation

Considering the hydrostatic approximation, the pressure ( $p$ ) at depth  $z$  can be obtained by integrating the vertical component of the equation of motion from  $z$  to the

free surface ( $\eta$ ):

$$p(x, y, z, t) = p_{\text{atm}} + g\rho_0\eta + g \int_z^0 \rho(x, y, z, t) dz. \quad (1)$$

Where the first term on the r.h.s is the atmospheric pressure at the sea surface, the second term is the pressure due to the free surface,  $\eta$ , displacement,  $\rho_0$  is the constant density value, and the last term on the r.h.s is the hydrostatic pressure (where  $\rho$  is density).

Introducing the separation (Eq. 1) requires the addition of a diagnostic or prognostic equation for  $\eta$ . Rigid lid models use different methods to solve the diagnostic problem for  $\eta$  (Dukowicz et al., 1993; Pinardi et al., 1995) but we will concentrate only on the prognostic formulation. The time-dependent equation for  $\eta$  is obtained by vertically integrating the continuity equation (under the incompressible approximation) and by applying surface and bottom dynamic boundary conditions:

$$\frac{\partial \eta}{\partial t} = -D + P + R - E \quad (2)$$

where

$$D = \nabla \cdot [(H + \eta) \bar{U}_h] \quad (3)$$

and

$$\bar{U}_h = \frac{1}{H + \eta} \int_{-H}^{\eta} \bar{u}_h dz \quad (4)$$

is the barotropic velocity field,  $\bar{u}_h$  the horizontal three dimensional velocity,  $H$  the bottom depth,  $P$  is the precipitation,  $R$  the runoff divided by the river cross-sectional area, and  $E$  the evaporation.

## Mediterranean sea level response to atmospheric pressure

P. Oddo et al.

[Title Page](#)

[Abstract](#)

[Introduction](#)

[Conclusions](#)

[References](#)

[Tables](#)

[Figures](#)

[⏪](#)

[⏩](#)

[◀](#)

[▶](#)

[Back](#)

[Close](#)

[Full Screen / Esc](#)

[Printer-friendly Version](#)

[Interactive Discussion](#)



The atmospheric pressure influences the horizontal velocity tendency which modifies the barotropic velocity field (Eq. 4), which in turn changes the horizontal divergence of the momentum (Eq. 3); the latter affects the  $\eta$  tendency (Eq. 2) which, again, modifies the total pressure.

Atmospheric pressure effects in numerical ocean models, especially when solving large scale problems, have often been neglected because of the relatively small amplitude of the horizontal gradients and the assumption that the major influence is almost stationary and can be computed by superimposing an inverse barometric effect on the free surface solution without atmospheric pressure. However, oceanic responses to atmospheric pressure forcing can depart from a pure inverse barometer effect under specific circumstances, especially in the presence of geometrical constraints (i.e. straits or channels) (Garrett and Majaess, 1984) as in the Mediterranean Sea (Le Traon and Gauzelin, 1997). Furthermore, coastal Kelvin waves or other fast barotropic waves can support or accelerate the barometric adjustment. Thus it is interesting to investigate how atmospheric pressure forcing influences the solution of primitive equations depending on the numerical schemes adopted to solve the prognostic Eq. (2).

The free-surface elevation response to atmospheric pressure may be composed of external gravity waves (EGWs). Their time scale is short compared to other processes described by primitive equations and thus they require a very small time step. Two methods are implemented in NEMO to allow a longer time step, solving the primitive equation in the presence of EGWs: the so-called *filtered* and *time-splitting* method (hereafter also referred to as FLT and TS, respectively).

NEMO users can decide between the two methods depending on the physical processes of interest. For fast EGWs, i.e. Poincaré or coastal Kelvin waves, then time-splitting is the most appropriate choice. If the focus is not on EGWs, a filter can be used to slow down the fastest waves while not altering the slow barotropic Rossby waves.

The filtering of EGWs in numerical models with a free surface is usually a matter of the discretisation of the temporal derivatives. In the NEMO code however, a slightly



the European Centre for Medium-Range Weather Forecasts (ECMWF) and model-predicted surface temperatures. Atmospheric pressure effects are not included in the model forcings. The natural surface boundary condition for vertical velocity is used.

Only seven major rivers were implemented (Fig. 1, upper panel): the Ebro, Nile and Rhone monthly values are from the Global Runoff Data Centre (Fekete et al., 1999), the Adriatic rivers Po, Vjose and Seman are from Raicich (Raicich, 1996) while the Bojana River climatological flow is taken from UNEP (1996). The Dardanelles inflow was parameterized as a river and its monthly climatological net inflow rates and salinity values were taken from Kourafalou and Barbopoulos (2003).

The advection scheme for active tracers is a mixed up-stream/MUSCL scheme (Monotonic Upwind Scheme for Conservation Laws, Van Leer, 1979, as implemented by Estubier and Levy, 2000). The up-stream scheme is used in proximity of the river mouths, in the Gibraltar Strait and close to the lateral open boundaries in the Atlantic. In Gibraltar, the up-stream scheme, together with an artificially increased vertical diffusivity, parameterizes the mixing that acts in this area due to the internal wave breaking, which is not explicitly resolved by the model.

In *NEMO-MFS-1*, the Atlantic box is nested within the monthly mean climatological fields computed from the daily output of the  $1/4^\circ$  global model (Drevillon et al., 2008), spanning from 2001 to 2005. The 2-D adaptive radiation condition (Marchesiello et al., 2001; Oddo and Pinardi, 2008) was used for the active tracers (temperature and salinity). Total velocities at the open boundaries are imposed by the global model solution, while barotropic velocities use a modified Flather (1976) lateral boundary condition explained in Oddo and Pinardi (2008). A summary of the model configuration is provided in Table 1, while details on the lateral open boundaries conditions are provided in Oddo et al. (2009).

Three additional NEMO configurations were created for this study. *NEMO-MFS-2* is identical to *NEMO-MFS-1* except for the inclusion of the atmospheric pressure forcing. This forcing, like the other atmospheric fields, is taken from ECMWF operational products. *NEMO-MFS-3* uses the time-splitting approach to solve the free surface elevation

## Mediterranean sea level response to atmospheric pressure

P. Oddo et al.

Title Page

Abstract

Introduction

Conclusions

References

Tables

Figures



Back

Close

Full Screen / Esc

Printer-friendly Version

Interactive Discussion



tendency Eq. (2), without considering the atmospheric pressure. Finally *NEMO-MFS-4* uses the time-splitting method and also takes into account the atmospheric pressure effects. The differences between the four model configurations are listed in Table 1 while Appendix A provides details on how to reproduce the physical setup used in this manuscript starting from the standard NEMO code.

All the simulations have been initialized with climatological temperature and salinity fields (SeaDataNet, [www.seadatanet.org](http://www.seadatanet.org)) on 7 January 2004 and ended on 31 December 2012.

## 4 Results and discussion

In this section the sensitivity of the circulation response due to the atmospheric pressure effect is analyzed as a function of the free surface elevation formulation in NEMO. Only the different solutions for  $\eta$  are considered since vertical profiles of temperature and salinity were not found to be significantly different among the four experiments. All the model configurations have very similar baroclinic skills to each other and to those ones obtained with similar NEMO experiments (Oddo et al., 2009).

To assess the accuracy of the model and to corroborate the numerical findings, sea level data retrieved from several tide gauges in the Mediterranean Sea were used (Fig. 1, bottom panel).

Since the Mediterranean's response to atmospheric pressure forcing varies according to the time scales considered (Garret and Majaess, 1984; Lascaratos and Gačić, 1990), model results are analyzed and discussed on the basis of different temporal scales. Firstly the low frequency response results are discussed in terms of model-to-model and models-to-observations comparisons in a period range spanning from the time-invariant components of the  $\eta$  signal up to 15 days. The high frequency model results are then analyzed in a period window from 15 days to 2 h.

## Mediterranean sea level response to atmospheric pressure

P. Oddo et al.

Title Page

Abstract

Introduction

Conclusions

References

Tables

Figures



Back

Close

Full Screen / Esc

Printer-friendly Version

Interactive Discussion



## 4.1 Low frequency components

The two-year mean component of the sea surface height (SSH) in the four experiments is shown in Fig. 2. At climatological time scales there are no significant differences between the two  $\eta$  numerical formulations, however qualitative differences in the circulation due to the introduction of pressure forcing are evident. The major Mediterranean circulation structures (Pinardi et al., 2013) are very similar among the various numerical model formulations but different due to the introduction of atmospheric pressure forcing. This forcing generally weakens all the cyclonic wind-driven structures as the atmospheric pressure forces  $\eta$  in the opposite way from the wind stress curl, i.e. the wind strengthens the cyclonic structures, whereas the associated atmospheric pressure weakens them. The Adriatic and the Rhode cyclonic gyre circulations illustrate the atmospheric pressure effects well, and the structures are more realistic in the atmospheric forcing cases.

The maps showing differences between the experiments with and without atmospheric pressure are also similar. A large-scale zonal gradient in the free surface is observed due to atmospheric pressure which produces higher  $\eta$  values in the Levantine basin and lower  $\eta$  values in the western Mediterranean Sea. Similar standard deviations maps (not shown) also indicate that, by introducing atmospheric pressure, the Levantine basin has larger seasonal oscillations than the remaining part of the Mediterranean Sea. In the various experiments, small-scale differences, i.e. eddy-like structures, were observed. These structures have horizontal scales that are much smaller than the atmospheric pressure scales and are probably due to the displacements of oceanic features as a consequence of instabilities induced by the new forcing.

A comparison between the time-series of daily values of  $\eta$  for the four experiments and corresponding observed data are shown in Fig. 3. Prior to the comparison, the steric effect was superimposed on the SSH model outputs, following Mellor and Ezer (1995). A time interval from July 2010 to July 2012 was selected, since a significant

GMDD

7, 3985–4017, 2014

### Mediterranean sea level response to atmospheric pressure

P. Oddo et al.

Title Page

Abstract

Introduction

Conclusions

References

Tables

Figures

⏪

⏩

◀

▶

Back

Close

Full Screen / Esc

Printer-friendly Version

Interactive Discussion



number of station data are available. Model results were first interpolated into the tide-gauge positions (Fig. 1, bottom panel) and then averaged.

The results were also evaluated by a power spectra comparison and coherency analysis with observations. For the coherency analysis smoothing was performed over eight adjacent frequencies. Results are shown for periods between 360 and 15 days because results for periods shorter than 15 days were shown to be sensitive to specific sampling positions and/or tide gauge locations (in agreement with Garret and Majaess 1984; Lascaratatos and Gačić 1990).

In agreement with Molcard et al. (2002) and Oddo et al. (2009) and irrespective of the experiment considered, both observational and modelled data are characterized by a large seasonal cycle modulated by inter-annual variability (the inter-annual variability is not shown since only a two-year interval series was selected from the model results in order to be consistent with the observational dataset available). Qualitatively, the longer time scales of the inter-annual variability have larger amplitudes in the winter than the summer. At very low frequencies the major difference in the results deriving from the two free surface methods is the amplitude of the seasonal cycle, i.e. the filtered formulation has a larger amplitude.

Comparing the power spectra (Fig. 3, left-middle panel), it is evident that the filtered formulation overestimates the energy content in the spectral window between 360 and 120 days. The introduction of the atmospheric pressure slightly reduces this model behaviour (Fig. 3, right-bottom panel). For shorter periods, between 120 and 15 days, the filtered formulation generally underestimates the energy content. Also in this case, by introducing the atmospheric pressure in the filtered formulation, there was a considerable improvement in the reproduction of the energy content.

Overall, the two experiments with the time-splitting formulation improved the reproduction of the observed energy content. At seasonal scales, the energy content is considerably lower than the filtered simulations and is closer to the observation. However in the window between 180 and 50 days, *NEMO-MFS-3* significantly underestimated

## GMDD

7, 3985–4017, 2014

### Mediterranean sea level response to atmospheric pressure

P. Oddo et al.

Title Page

Abstract

Introduction

Conclusions

References

Tables

Figures



Back

Close

Full Screen / Esc

Printer-friendly Version

Interactive Discussion



the observed variability due to the missing contribution of atmospheric pressure in this period range.

At frequencies between 120 and 15 days<sup>-1</sup> *NEMO-MFS-3* and *NEMO-MFS-1* without atmospheric pressure forcing have very similar energy contents and both underestimated the observed values.

As for the filtered formulation, by introducing the atmospheric pressure in the time splitting experiments, the energy content of  $\eta$  increases in the spectral window between 120 and 15 days, reaching generally closer values to the observations. In terms of energy content, introducing the atmospheric pressure has a significant impact for periods shorter than 120/100 days (see the gain panel in Fig. 3). For periods longer than 120/100 days, the numerical scheme used to solve Eq. (2) plays a major role in determining the ocean dynamic (irrespective of the additional forcing introduced), while for periods shorter than 120/100 days, the effect of atmospheric pressure dominates over the effect of the specific numerical solution method for  $\eta$ .

In all the experiments, the coherence is fairly high (Fig. 3, right middle panel). There were significant improvements with the introduction of the atmospheric pressure, irrespective of the numerical solution methods, for periods longer than 50 days. The phase difference is always small and generally below 30°. There was a significant phase shift between observations and model simulation values between 40 and 25 days in the absence of atmospheric pressure forcing. For periods shorter than 180 days, all the gains are generally smaller than 1, which means that the model underestimated the amplitude of  $\eta$  oscillations. However there was a significant improvement by introducing the atmospheric pressure forcing for periods shorter than 50 days.

The analysis so far was performed for the model and observed average sea level at the 25 tide gauge stations (Fig. 1). This can be considered as a good estimate of the mean sea level of the Mediterranean Sea because no significant differences were observed, at these time scales, averaging over the whole Mediterranean Sea or by only sampling at tide gauge locations.

**Mediterranean sea level response to atmospheric pressure**

P. Oddo et al.

Title Page

Abstract

Introduction

Conclusions

References

Tables

Figures



Back

Close

Full Screen / Esc

Printer-friendly Version

Interactive Discussion







Fig. 1 (bottom panel). The Mediterranean's response to atmospheric pressure varies spatially, as different processes characterize different areas of the basin. Prior to the comparison, the tidal signal was removed from the observed dataset and steric effect superimposed on model results. Modelled and observed sea level data time-series were also compared by analyzing individual power spectra.

In Fig. 6 the sea level time-series (top panel) and power spectrum (bottom panel) are shown for the station in Valencia. At relatively low frequencies (lower than  $240 \text{ h}^{-1}$ ), the experiments without the atmospheric pressure underestimated the amplitude of the oscillations. In the range between 5 (120 h) and 1.5 days all the experiments performed in a similar way, slightly underestimating the observed sea level variability. Differences between model results are more evident for periods lower than 24 h. For these periods (lower than 24 h), differences between numerical schemes and additional forcing effects are more evident. Experiments without the atmospheric pressure forcing, *NEMO-MFS-1* and *NEMO-MFS-3*, strongly underestimated the amplitude of the signal. By introducing the atmospheric pressure, the energetic level increased in both *NEMO-MFS-2* and *NEMO-MFS-4*. In addition, by introducing the atmospheric pressure, generally the time-splitting formulation improved the reproduction of the energetic content of the observed signals, although it tended to overestimate the 4 h oscillation.

The use of the time-splitting formulation and the introduction of the atmospheric pressure (*NEMO-MFS-4*) produced significantly different model results from the other simulations for periods shorter than 6 h. These very high frequency oscillations are evident in the observed time-series and represent the main difference between the sea level observed in Mahon (Fig. 7) and in Valencia. These oscillations also have a higher frequency than the atmospheric forcing used in the simulations ( $6 \text{ h}^{-1}$ ), thus we argue that some high frequency barotropic processes excited by the introduction of the atmospheric pressure forcing may interact with bathymetry (the narrow continental shelf in front of Valencia) and background velocities, resulting in very high frequency barotropic waves. This is evident when comparing the different power spectra for the

## Mediterranean sea level response to atmospheric pressure

P. Oddo et al.

Title Page

Abstract

Introduction

Conclusions

References

Tables

Figures

◀

▶

◀

▶

Back

Close

Full Screen / Esc

Printer-friendly Version

Interactive Discussion





energetic levels between *NEMO-MFS-1* and *NEMO-MFS-2* were similar. On the other hand the differences in power spectra between *NEMO-MFS-3* and *NEMO-MFS-4* were significant, reaching a relative maximum at a  $4 \text{ h}^{-1}$  frequency.

## 5 Summary and conclusions

The sensitivity of the Mediterranean Sea ocean dynamics to the free surface elevation numerical formulation in NEMO was evaluated for cases with and without atmospheric pressure forcings. Four different NEMO configurations were created and the results compared with each other and with available observations. All the NEMO configurations were implemented using the same horizontal and vertical meshes.

The reference NEMO configuration, *NEMO-MFS-1*, uses a filtered formulation of the free surface equation (Roullet and Madec, 2000) and does not take into account the atmospheric pressure effects. This model setup is currently used in the framework of the Mediterranean Forecasting System (Pinardi and Flemmings, 1989).

*NEMO-MFS-2* differs from *NEMO-MFS-1* due to the introduction of the atmospheric pressure forcing. The free surface equation is solved using a time-splitting approach (Griffies, 2004) which either does or does not account for the atmospheric pressure effect in *NEMO-MFS-3* and *NEMO-MFS-4* configurations, respectively.

The spatial variability induced by the introduction of the atmospheric pressure in the two-year mean component of the *sea level* was not influenced by the different numerical formulations used to solve the free surface equation (Fig. 2). However the introduction of the atmospheric pressure induced a basin scale zonal sea level negative gradient (higher values in the east and lower in the west) and a weakening of all the cyclonic wind-driven structures irrespectively of the free surface formulation adopted. The structure of the sea level and the corresponding circulation could be considered as more realistic with atmospheric pressure forcing although observational evidence is lacking at the basin scale.



## Mediterranean sea level response to atmospheric pressure

P. Oddo et al.

Title Page

Abstract

Introduction

Conclusions

References

Tables

Figures

◀

▶

◀

▶

Back

Close

Full Screen / Esc

Printer-friendly Version

Interactive Discussion



An interesting finding of this study is the effect of the numerical scheme on the phase shift between Gibraltar transport and surface mass fluxes. This phase shift modulated the  $\eta$  seasonal oscillation differently in the four experiments. The main differences in the four experiments derive from the introduction of the time splitting formulation, while atmospheric pressure forcing plays a minor role in modulating the phase of the two signals at seasonal scales. The phase shift produced using time-splitting amplifies the phase opposition between surface mass fluxes and the Gibraltar transport, and the resulting stochastic component of the sea level tendency has a smaller amplitude.

An analysis of the observed and modelled high frequencies datasets in three different locations in the Mediterranean Sea (although two locations are relatively close to each other: Valencia and Mahon) highlights that the interaction between atmospheric pressure and barotropic dynamics follows different dynamics. In Mahon, an open ocean station in the western Mediterranean Sea (Fig. 1, bottom panel), the introduction of the atmospheric pressure forcing in the model represents the fundamental step in reproducing the observed  $\eta$  variability and energetic content. In Venice, located in the northernmost part of a semi-enclosed basin and characterized by very shallow water, the introduction of the atmospheric pressure clearly enabled the models to correctly simulate the seiches which are also driven by the atmospheric pressure differences between the north and south Adriatic. However it is the explicit resolution of the barotropic processes (using the time-splitting) that allows the model to correctly simulate the  $\eta$  dynamics at high frequencies. Finally in Valencia, it is the combination of both the atmospheric pressure and the time splitting, that enabled the model to reach the correct energetic levels at high frequencies.

### Appendix A:

The NEMO model is freely available under the CeCILL public license. After registering at the NEMO website (<http://www.nemo-ocean.eu>), users should follow the procedure described in the “NEMO Quick Start Guide” section to access and run the model.



## Mediterranean sea level response to atmospheric pressure

P. Oddo et al.

[Title Page](#)

[Abstract](#)

[Introduction](#)

[Conclusions](#)

[References](#)

[Tables](#)

[Figures](#)

[⏪](#)

[⏩](#)

[◀](#)

[▶](#)

[Back](#)

[Close](#)

[Full Screen / Esc](#)

[Printer-friendly Version](#)

[Interactive Discussion](#)



Ferry, N., Hernandez, F., Le Galloudec, O., Messal, F., and Parent, L.: The GODAE/Mercator-Ocean global ocean forecasting system: results, applications and prospects, *J. Operational Oceanogr.*, 1, 51–57, 2008.

Dukowiz, J. K., Smith, R. D., and Malone, R. C.: A reformulation and implementation of the Bryan–Cox–Semtner ocean model on the connection machine, *J. Atmos. Ocean. Tech.*, 10, 2, 195–208, 1993.

Estubier, A. and Levy, M.: Quel schema numerique pour le transport d'organismes biologiques par la circulation oceanique, Note Techniques du Pole de modelisation, Institut Pierre-Simon Laplace, 81 pp., 2000.

Fekete, B. M., Vorosmarty, C. J., and Grabs, W.: Global, composite runoff fields based on observed river discharge and simulated water balances, Tech. Rep. 22, Global Runoff Data 25 Cent., Koblenz, Germany, 1999.

Flather, R. A.: A tidal model of the northwest European continental shelf, *Memories de la Societe Royale des Sciences de Liege*, 6, 141–164, 1976.

Garrett, C. J. R.: Variable sea level and strait flows in the Mediterranean: a theoretical study of the response to meteorological forcing, *Oceanol. Acta*, 6, 79–87, 1983.

Garrett, C. J. R. and Majaess, F.: Nonisostatic response of sea level to atmospheric pressure in the Eastern Mediterranean, *J. Phys. Oceanogr.*, 14, 656–665, 1984.

Godin, G. and Trotti, L.: Trieste-water levels 1952–1971: A study of the tide, mean level and seiche activity, Environment Canada, Fisheries and Marina Services, Miscellaneous Special Publication, Dept. of the Environment, Fisheries and Marine Service in Ottawa, 28, 1975.

Griffies, S. M.: *Fundamentals of Ocean Climate Models*, Princeton University Press, 434 pp., 2004.

Kasumović, M.: On the influence of air pressure and wind on the Adriatic Sea level fluctuations, *Hydrografski godišnjak*, 1956/57, 107–121, 1958 (in Croatian).

Kourafalou, V. H. and Barbopoulos, K.: High resolution simulations on the North Aegean Sea seasonal circulation, *Ann. Geophys.*, 21, 251–265, doi:10.5194/angeo-21-251-2003, 2003.

Lacombe, H.: Contribution à l'étude du détroit de Gibraltar, étude de dynamique, *Cah. Océanogr.*, 12, 73–107, 1961.

Lascaratos, A. and Gačić, M.: Low-frequency sea level variability in the northeastern Mediterranean, *J. Phys. Oceanogr.*, 20, 522–533, 1990.

Le Traon, P. Y. and Gauzelin, P.: Response of the Mediterranean mean sea level to atmospheric pressure forcing, *J. Geophys. Res.*, 102, 973–984, 1997.



## Mediterranean sea level response to atmospheric pressure

P. Oddo et al.

Title Page

Abstract

Introduction

Conclusions

References

Tables

Figures

⏪

⏩

◀

▶

Back

Close

Full Screen / Esc

Printer-friendly Version

Interactive Discussion



phase of implementation (1998–2001), *Ann. Geophys.*, 21, 3–20, doi:10.5194/angeo-21-3-2003, 2003.

Pinardi, N., Zavatarelli, M., Adani, M., Coppini, G., Fratianni, C., Oddo, P., Simoncelli, S., Tonani, M., Lyubartsev, V., Dobricic, S., and Bonaduce, A.: Mediterranean Sea large-scale low-frequency ocean variability and water mass formation rates from 1987 to 2007: a retrospective analysis, *Prog. Oceanogr.*, doi:10.1016/j.pocean.2013.11.003, in press, 2013.

Pinardi, N., Bonaduce, A., Navarra, A., Dobricic, S., and Oddo, P.: The mean sea level equation and its application to the Mediterranean sea, *J. Climate*, 27, 442–447, doi:10.1175/JCLI-D-13-00139.1, 2014.

Ponte, R. M.: Variability in a homogeneous global ocean forced by barometric pressure, *Dynam. Atmos. Oceans*, 18, 209–234, 1993.

Raicich, F.: On fresh water balance of the Adriatic Sea, *J. Marine Syst.*, 9, 305–319, 1996.

Roulet, G. and Madec, G.: Salt conservation, free surface, and varying levels: a new formulation for ocean general circulation models, *J. Geophys. Res.*, 105, 23927–23942, 2000.

Torrence, C. and Compo, G. P.: A practical guide to wavelet analysis, *B. Am. Meteorol. Soc.*, 79, 61–78, 1998.

UNEP: Implications of Climate Change for the Albanian Coast, Mediterranean Action Plan, MAP Technical Reports Series No. 98., 1996.

Van Leer, B.: Towards the ultimate conservative difference scheme, V. A second order sequel to Godunov's method, *J. Com. Phys.*, 32, 101–136, 1979.

Wunsch, C.: Bermuda sea level in relation to tides, weather and baroclinic fluctuations, *Rev. Geophys. Space Ge.*, 10, 1–49, doi:10.1029/RG010i001p00001, 1972.

**Table 1.** NEMO–MFS configurations with corresponding cpp keys and namelist variables.

	NEMO			
	MFS-1	MFS-2	MFS-3	MFS-4
Horiz. Resolution	1/16 Degree			
Vertical Discretization	72 z levels with partial cells. ( <i>ln_zps = .true.</i> )			
Horiz. Viscosity	Bi-Laplacian $A_{mh} = -5e.9 \text{ m}^4 \text{ s}^{-1}$ ( <i>ln_dynldf_bilap = .true.</i> )			
Horiz. Diffusivity	Bi-Laplacian $A_{th} = -3.e9 \text{ m}^4 \text{ s}^{-1}$ ( <i>ln_traldf_bilap = .true.</i> )			
Vertical Visc. scheme	Pacanowski & Philander ( <i>key_zdfrc</i> )			
Free-surface formulation	Filtered ( <i>key_dynspg_ftt</i> )		Time-Splitting ( <i>key_dynspg_ts</i> )	
Time-step	600 s		Number of barotropic sub-time steps <i>nn_baro</i> = 100	
Initial Condition	MedAtlas Climatology			
Air-sea fluxes	MFS-Bulk formulae ( <i>ln_blk_mfs = .true.</i> )			
Atmospheric press.	No	Yes	No	Yes
<i>ln_apr_dyn =</i>	<i>.false.</i>	<i>.true.</i>	<i>.false.</i>	<i>.true.</i>
Runoff	As Surface boundary condition for S and w ( <i>ln_rnf = .true.</i> )			
Solar radiation	2 Bands Penetration ( <i>ln_qsr_2bd = .true.</i> )			
Lateral momentum B.C.	No-sleep ( <i>rn_shlat = 2.</i> )			
Bottom momentum B.C	Non linear friction ( <i>nn_bfr = 2</i> )			
EOS	UNESCO – Jackett and McDougall (1994) ( <i>nn_eos = 0</i> )			
Tracer Advection	Up-stream/MUSCL ( <i>ln_traadv_muscl = .true.</i> )			
	Vector form (energy and enstrophy cons. scheme)			
Momentum Advection	( <i>ln_dynadv_vec = .true.</i> <i>ln_dynvor_eeen = .true.</i> )			
Back. Vertical Visc.	$A_{mv} = 1.2e-5 \text{ m}^2 \text{ s}^{-1}$			
Back. Vertical Diff.	$A_{tv} = 1.2e-6 \text{ m}^2 \text{ s}^{-1}$			
Vertical visc/diff Scheme	Implicit ( <i>ln_zdfexp = .false.</i> )			

## Mediterranean sea level response to atmospheric pressure

P. Oddo et al.

Title Page

Abstract

Introduction

Conclusions

References

Tables

Figures



Back

Close

Full Screen / Esc

Printer-friendly Version

Interactive Discussion



**Table A1.** Namelist.

	GYRE	MFS-1	MFS-2	MFS-3	MFS-4
In_zco	true			false	
In_zps	false			true	
In_ana	true			false	
In_blk_mfs	false			true	
In_rnf	false			true	
In_bfrimp	true			false	
nn_eos	2			0	
In_traadv_tvd	true			false	
In_traadv_muscl	false			true	
In_traldf_lap	true			false	
In_traldf_bilap	false			true	
In_traldf_hor	false			true	
In_traldf_iso	true			false	
In_hpg_zco	true			false	
In_hpg_zps	false			true	
In_dynldf_lap	true			false	
In_dynldf_bilap	false			true	
rn_ahm_0_blp	0			$-5 \times 10^9$	
rn_ahm_0	1000			$-3 \times 10^9$	
In_apr_dyn	false	false	false	true	true

## Mediterranean sea level response to atmospheric pressure

P. Oddo et al.

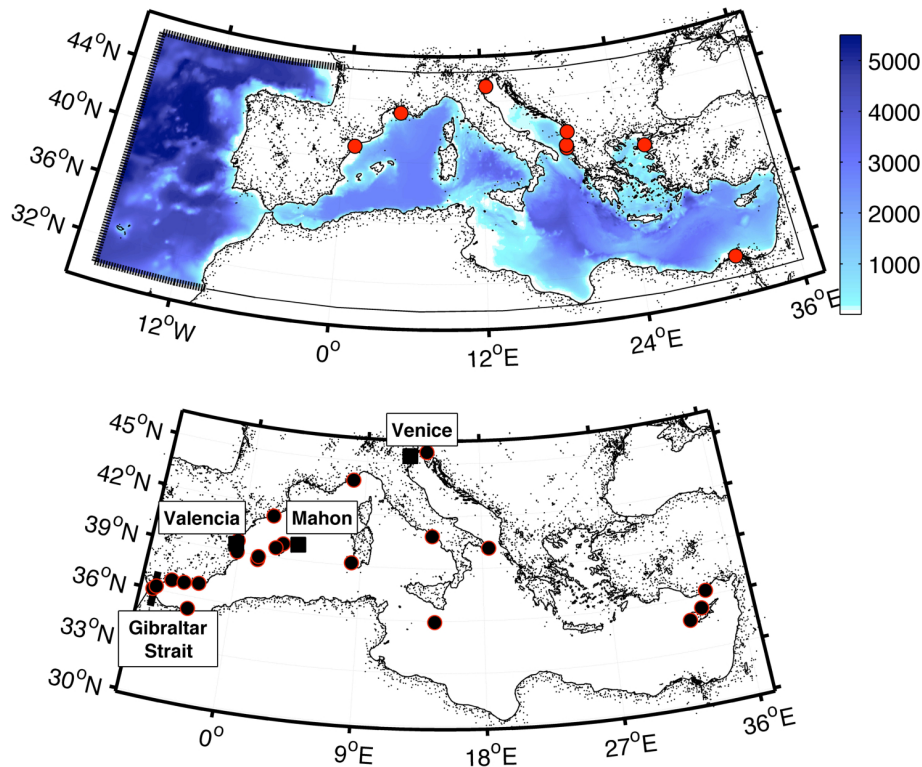


**Figure 1.** Upper Panel: model domain. Bold dashed lines in the Atlantic indicate the location of the lateral boundaries of the model. Red circles indicate river locations and Dardanelles inflow. Bottom Panel: black circles indicate tide gauge positions. Dark squares indicate the positions of the tide gauges collecting high frequency data. The Gibraltar Strait is also shown.

[Title Page](#)[Abstract](#)[Introduction](#)[Conclusions](#)[References](#)[Tables](#)[Figures](#)[⏪](#)[⏩](#)[◀](#)[▶](#)[Back](#)[Close](#)[Full Screen / Esc](#)[Printer-friendly Version](#)[Interactive Discussion](#)

## Mediterranean sea level response to atmospheric pressure

P. Oddo et al.

Title Page

Abstract

Introduction

Conclusions

References

Tables

Figures

◀

▶

◀

▶

Back

Close

Full Screen / Esc

Printer-friendly Version

Interactive Discussion

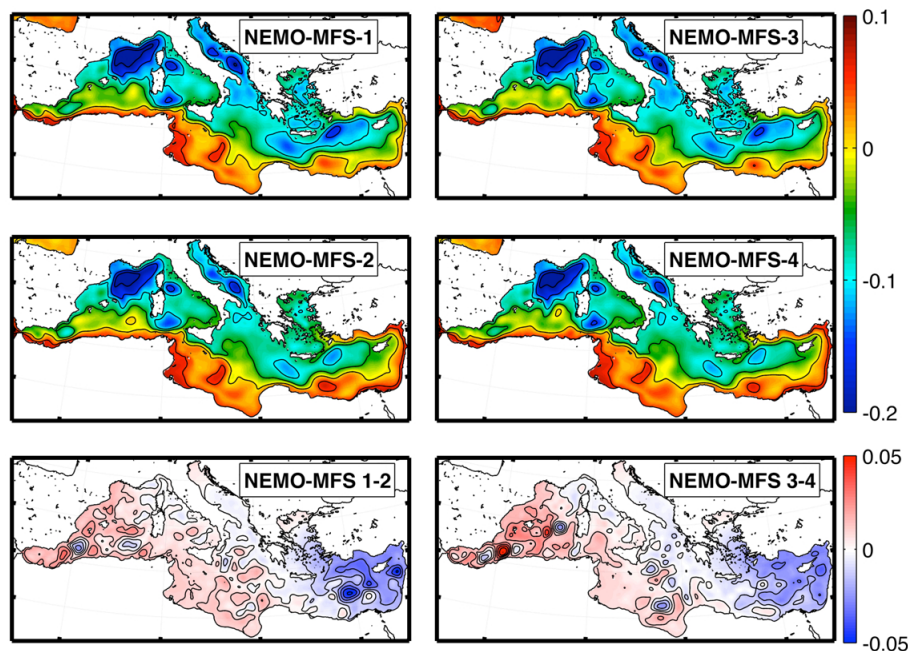


**Figure 2.** Horizontal maps of the two-year mean component of the sea surface elevation in the four experiments (units are meters). The two bottom panels represent the sea surface elevation differences between the experiments with and without atmospheric pressure forcing for the time-splitting (right) and the filtered free surface (left) cases.

## Mediterranean sea level response to atmospheric pressure

P. Oddo et al.

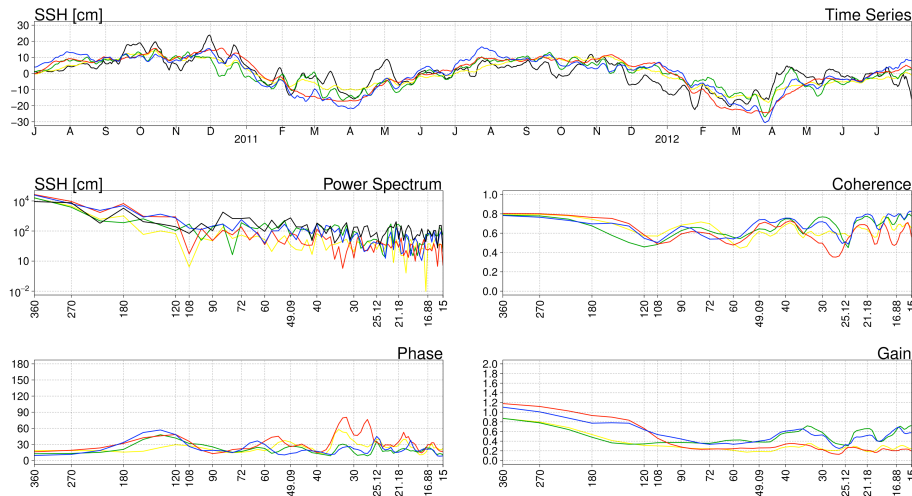


**Figure 3.** Top panel: Mediterranean mean sea level time-series from the four experiments and observations averaged over the tide gauge positions shown in Fig. 1. The black line represents observational data, the red line represents NEMO-MFS-1 results, the blue line represents NEMO-MFS-2 results, the yellow line represents NEMO-MFS-3 results, and the green line represents NEMO-MFS-4 results. Left middle panel:  $\eta$  power spectra for observations and model results, units are cm<sup>2</sup>. Right middle, left bottom and right bottom panels: coherence, phase (degrees) and gain computed between observations and model, respectively. Units in the x axis are periods in days.

[Title Page](#)
[Abstract](#)
[Introduction](#)
[Conclusions](#)
[References](#)
[Tables](#)
[Figures](#)
[Back](#)
[Close](#)
[Full Screen / Esc](#)
[Printer-friendly Version](#)
[Interactive Discussion](#)

## Mediterranean sea level response to atmospheric pressure

P. Oddo et al.

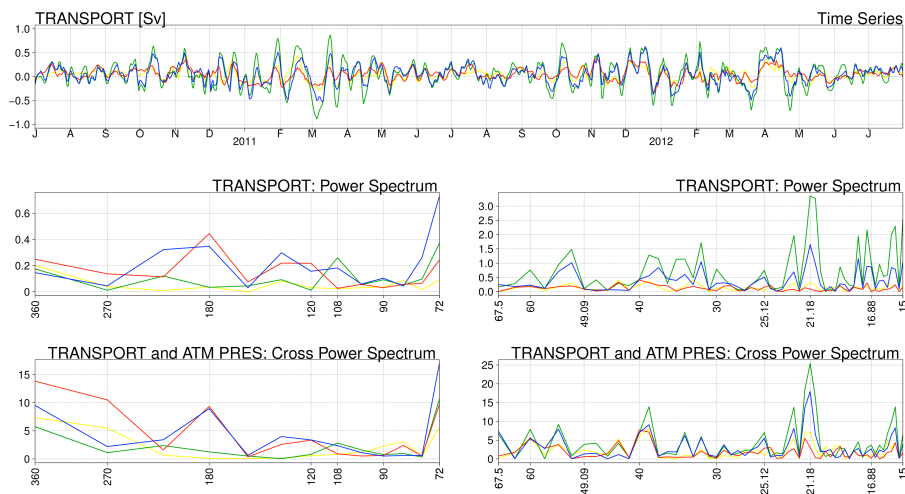


**Figure 4.** (Top panel) Gibraltar transport time-series from the four experiments. Middle panels: Gibraltar transport power spectra. The period axes are separated to better display the energy content. Bottom panels: cross power spectrum between Gibraltar transport and atmospheric pressure. Colours as in Fig. 3.

Title Page

Abstract

Introduction

Conclusions

References

Tables

Figures



Back

Close

Full Screen / Esc

Printer-friendly Version

Interactive Discussion



## Mediterranean sea level response to atmospheric pressure

P. Oddo et al.

Title Page

Abstract

Introduction

Conclusions

References

Tables

Figures

◀

▶

◀

▶

Back

Close

Full Screen / Esc

Printer-friendly Version

Interactive Discussion

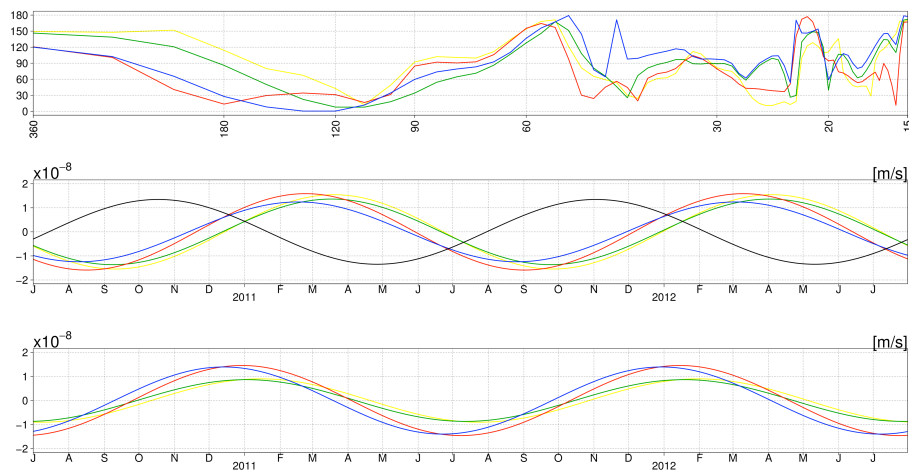


**Figure 5.** Top panel: phase analysis between Gibraltar transport and surface mass fluxes. Middle panel: Gibraltar transport for the four experiments and surface mass flux reconstructed using only seasonal frequencies. The solid dark line indicates the surface mass fluxes, coloured lines indicate model results as in Fig. 3. Bottom panel: seas surface height stochastic component for the four experiments reconstructed using only seasonal frequencies.

**Mediterranean sea  
level response to  
atmospheric  
pressure**

P. Oddo et al.

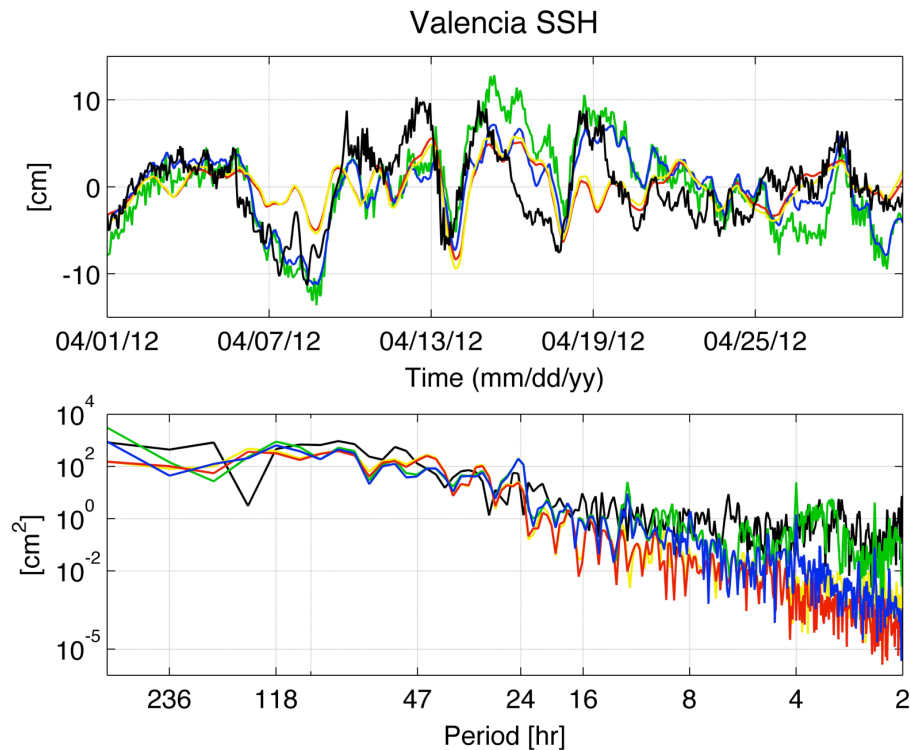


**Figure 6.** Valencia sea surface elevation time-series (Top panels) from observations and models results, and corresponding power spectrum (Bottom panel). Colours as in Fig. 3.

Mediterranean sea  
level response to  
atmospheric  
pressure

P. Oddo et al.

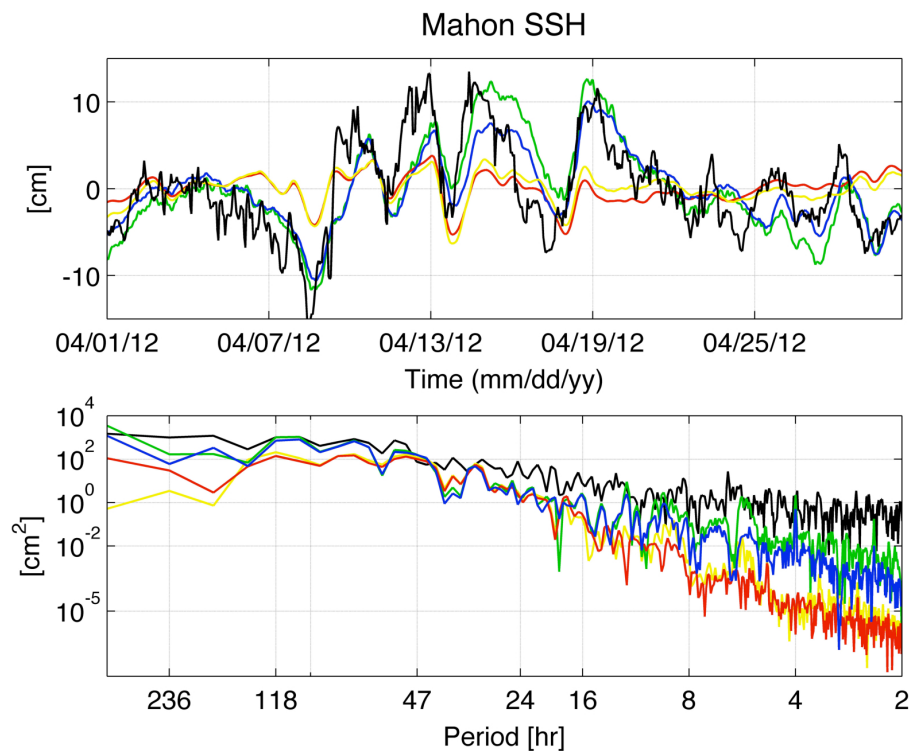


**Figure 7.** Mahon  $\eta$  time-series (Top panels) from observations and model results, and corresponding power spectrum (Bottom panel). Colours as in Fig. 3.

## Mediterranean sea level response to atmospheric pressure

P. Oddo et al.

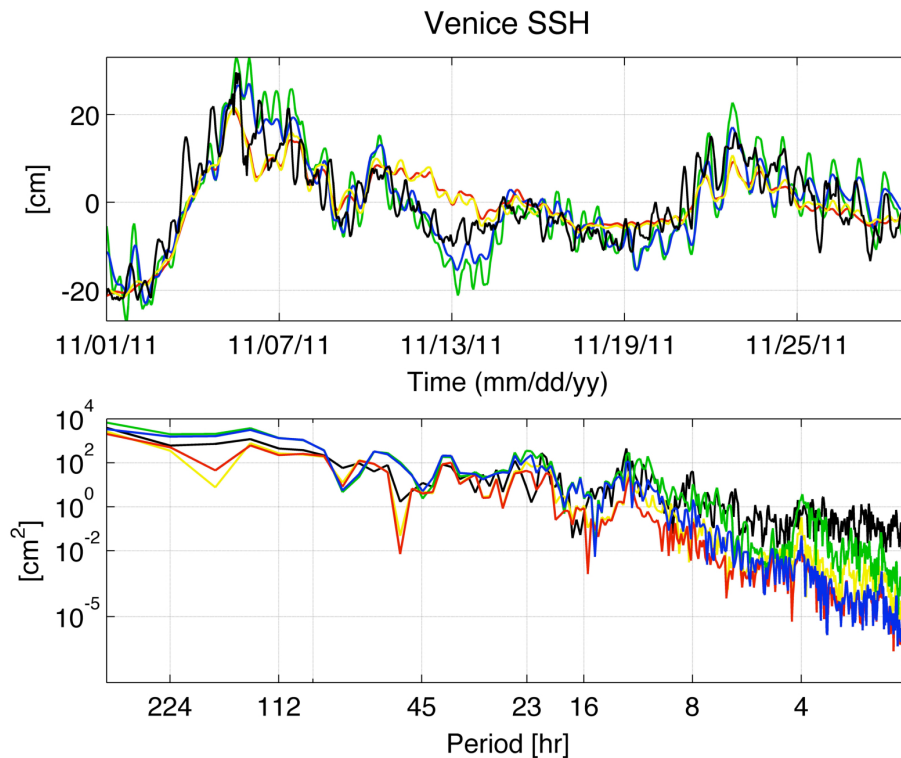


**Figure 8.** Venice  $\eta$  time-series (Top panels) from observations and model results, and corresponding power spectrum (Bottom panel). Colours as in Fig. 3.